




## Article

# MCM-41-Type Mesoporous Silicas Modified with Alumina in the Role of Catalysts for Methanol to Dimethyl Ether Dehydration

Natalia Szczepanik, Andrzej Kowalczyk , Zofia Piwowska  and Lucjan Chmielarz \* 

Faculty of Chemistry, Jagiellonian University, Gronostajowa 2, 30-387 Kraków, Poland

\* Correspondence: chmielar@chemia.uj.edu.pl; Tel.: +48-12-686-24-17

**Abstract:** MCM-41-type mesoporous silicas were modified with alumina by the impregnation, co-condensation, and template ion-exchange (TIE) methods. The obtained materials were characterized with respect to their chemical composition (ICP-OES), textural parameters (low-temperature N<sub>2</sub> sorption), structure (XRD), and surface acidity (NH<sub>3</sub>-TPD) and tested as catalysts of methanol to dimethyl ether (DME) dehydration in a flow microreactor system. The catalytic performance of the studied materials was analyzed with respect to their porous structure, as well as their density and the strength of their acid sites. It was shown that the performance of the studied catalysts depends on the contribution of the surface exposed aluminum species, as well as their aggregation. For the most active catalyst, the study of its catalytic stability under reaction conditions was performed. It was shown that the catalyst can be effectively regenerated by the incineration of carbon deposits under air flow at 550 °C for 1 h.

**Keywords:** methanol to dimethyl ether dehydration; MCM-41; alumina; surface acidity; catalyst regeneration



**Citation:** Szczepanik, N.; Kowalczyk, A.; Piwowska, Z.; Chmielarz, L. MCM-41-Type Mesoporous Silicas Modified with Alumina in the Role of Catalysts for Methanol to Dimethyl Ether Dehydration. *Catalysts* **2022**, *12*, 1324. <https://doi.org/10.3390/catal12111324>

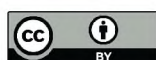
Academic Editors: Angela Martins and Ana Paula Carvalho

Received: 1 October 2022

Accepted: 20 October 2022

Published: 27 October 2022

**Publisher's Note:** MDPI stays neutral with regard to jurisdictional claims in published maps and institutional affiliations.



**Copyright:** © 2022 by the authors. Licensee MDPI, Basel, Switzerland. This article is an open access article distributed under the terms and conditions of the Creative Commons Attribution (CC BY) license (<https://creativecommons.org/licenses/by/4.0/>).

## 1. Introduction

Dimethyl ether, DME, is considered a clean and environmentally friendly fuel that could be an alternative to diesel fuel, owing to its high cetane number, low autoignition temperature, and reduced emissions. Since there is no C-C bond in the DME molecule, the formation of carbon nanoparticles during its combustion is effectively limited. DME can be used in specially designed compression ignition diesel engines [1]. Moreover, DME fuel can be safely stored because the ether will not form explosive peroxide [2]. There are two main technologies used for the DME production. The first one, called STD-syngas-to-dimethyl ether, is based on the conversion of syngas (CO + H<sub>2</sub>) to DME. In this case, the bifunctional catalyst, active in the syngas to methanol conversion, as well as in the methanol to DME dehydration process, is used [3–5]. In the second technology, the DME production is split into two reactions, conducted separately. In the first reaction, syngas is converted to methanol, while in the second reaction, after purification, methanol is dehydrated to DME. The conversion of methanol to DME is called the MTD (methanol-to-dimethyl ether) process [6,7]. The MTD process requires an acidic solid catalyst, such as  $\gamma$ -Al<sub>2</sub>O<sub>3</sub> [8], zeolites [9], or modified clay minerals [10,11], as well as heteropolyacids [12,13]. Thus, the number of acid sites, as well as their relative strength, are crucial parameters determining the catalyst performance in the MTD process. Acid sites that are too weak are unable to properly activate methanol molecules to be converted to DME [14], while acid sites that are too strong may result in the rapid formation of carbon deposits, thus decreasing the efficiency of the DME formation [15]. A high concentration of acidic sites can be obtained by the deposition of additional components, e.g., aluminum [11], forming such sites on high-surface area supports. Mesoporous silica materials, among other porous materials such as MXenes [16] and carbon nanotubes [17], belong to a group of porous materials

with great, but still not fully used, potential. Mesoporous silica materials, such as MCM-41, are excellent supports of the MTD catalysts, due to their very high surface area, uniform pore size in the mesopore range, and relatively good thermal and hydrothermal stability. A large number of acid sites, catalytically active in the MTD process, can be formed on a very large surface area of such silica materials. On the other hand, relatively large and uniform pores result in a very effective internal diffusion of the reactants inside the pores. Therefore, the overall efficiency of DME formation in the presence of mesoporous silica, including MCM-41, should be very high. However, due to lack of surface acidity, such pure silica mesoporous materials do not exhibit any catalytic activity in methanol dehydration (Supplementary Materials, Figure S1), and therefore, such materials must be modified to create surface acid sites. The acid sites can be generated by the deposition of alumina on a very large surface area of mesoporous silica materials, which should result in the formation of a large number of such acid sites; these play a crucial catalytic role in methanol-to-DME dehydration. The selection of an appropriate aluminum source and method of deposition is important for the generation of acid sites of suitable strength, as well as high surface density. In addition to co-condensation and impregnation, the template ion-exchange (TIE) method, based on the replacement of alkylammonium cations in freshly prepared mesoporous silica (non-calcined) for metal cations, also seems to be very promising [18,19]. The TIE method was successfully applied for the deposition for various metals, including copper, iron, or magnesium, into MCM-41-type mesoporous silica in both cylindrical and spherical forms [20,21]. To obtain high dispersion of introduced metal species, the conditions regarding the TIE procedure, such as type of metal precursors, their concentrations [22], and the solvent used [18], are all very important.

The catalysts for the MTD process, based on mesoporous MCM-41-type silica material modified with aluminum by three different methods—co-condensation, impregnation, and TIE—are presented, compared, and discussed.

## 2. Results and Discussion

MCM-41-type mesoporous silica, modified with aluminum by the impregnation (IMP), co-condensation (CC), and template ion-exchange (TIE) methods, were characterized with respect to their structure, texture, chemical composition, and surface acidity and tested as catalysts of methanol to DME conversion. In the sample code *XAl-MET*, *X* is related to the intended aluminium loadings (1, 2, or 3 wt.%), while *MET* indicates the method used for aluminum deposition (IMP—impregnation, CC—co-condensation, TIE—template ion-exchange).

X-ray diffractograms recorded for the samples with the highest content of aluminum deposited by different methods are shown in Figure 1.

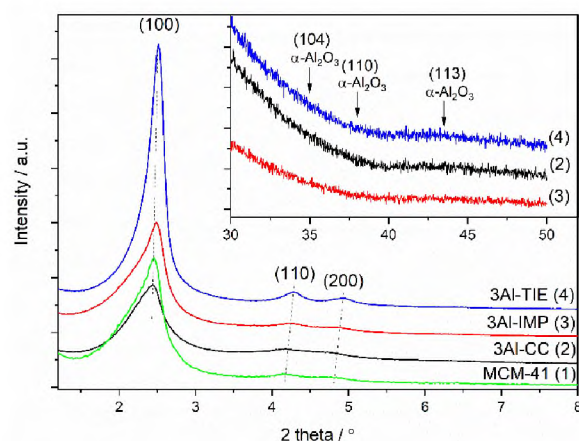


**Figure 1.** X-ray diffractograms of MCM-41 modified with aluminum using different methods.



In the diffractogram of all studied samples three reflections, (100), (110), and (200), characteristic of the hexagonal structure of MCM-41, are present (Figure 1). Thus, in the case of all samples, independent of the method used for their synthesis or modification, the porous structure typical of MCM-41 was obtained. There is a significant difference between the intensities of the reflections. The less intensive reflections noted in the diffractogram of the samples obtained by the co-condensation method show that the incorporation of heteroatoms into the silica walls of MCM-41 decreased the pore ordering in this type of mesoporous silica. This effect has previously been reported in the literature [23]. There is a significant difference in the intensity of the reflections in the diffractograms of pure silica MCM-41 and the samples obtained by the impregnation and TIE methods. In the case of the sample produced by the impregnation method, prior to the aluminum deposition, mesoporous silicas containing organic surfactants inside the pores were calcined (sample MCM-41, Figure 1). The incineration of such organic compounds under calcination conditions produced a large amount of heat (exothermic process), which could result in local overheating of the samples and partial distortion of the ordered porous structure. In the case of the samples modified by the TIE method a significant number of organic surfactants was removed from the pore system of MCM-41 during the template ion-exchange procedure. Therefore, the risk of the sample overheating, as well as the destruction of their porous structure, was significantly limited. The reflections characteristic of  $\text{Al}_2\text{O}_3$  phases- $\gamma$ - $\text{Al}_2\text{O}_3$  (JCPDS 10-0425) and  $\delta$ - $\text{Al}_2\text{O}_3$  (JCPDS 00-016-0394) were not found in the diffractograms of the studied samples (Figure 1, insert), showing that aluminum was deposited into MCM-41 in relatively highly dispersed forms.

The content of aluminum in the samples is presented in Table 1. As can be seen, the real content of aluminum in the series of the samples obtained by the co-condensation method is significantly lower compared to the intended aluminum contents (1, 2, and 3 wt.%) in MCM-41. This effect can be explained by the lower reactivity of the aluminum source (AIP) in comparison to the silica source (TEOS). The real aluminum contents in the samples obtained by the impregnation method are very close to the intended values, while in the silicas modified with aluminum using the TIE method, the measured content of this metal is slightly higher than the intended values.

**Table 1.** Chemical composition, textural parameters, and surface concentration of acid sites.

Sample	Si/Al [mol·mol <sup>-1</sup> ]	Al Content* [wt.%]	S <sub>BET</sub> [m <sup>2</sup> ·g <sup>-1</sup> ]	Pore Volume [cm <sup>3</sup> ·g <sup>-1</sup> ]	C <sub>A</sub> [μmol·g <sup>-1</sup> ]	C <sub>A</sub> /Al [mol·mol <sup>-1</sup> ]
MCM-41	-	0.00	1171 (±59)	0.87 (±0.05)	-	-
1Al-CC	83	0.52	1125 (±56)	0.99 (±0.05)	39 (±1)	0.20
2Al-CC	44	1.00	1123 (±56)	0.96 (±0.05)	62 (±2)	0.17
3Al-CC	28	1.43	1173 (±59)	1.03 (±0.05)	69 (±2)	0.13
1Al-IMP	44	0.97	1055 (±53)	0.76 (±0.04)	63 (±2)	0.18
2Al-IMP	21	1.92	1026 (±51)	0.79 (±0.04)	100 (±2)	0.14
3Al-IMP	15	2.88	997 (±50)	0.76 (±0.04)	143 (±4)	0.13
1Al-TIE	36	1.13	1128 (±56)	0.97 (±0.05)	141 (±4)	0.34
2Al-TIE	18	2.50	1082 (±54)	0.95 (±0.05)	243 (±6)	0.26
3Al-TIE	13	3.21	1043 (±52)	0.91 (±0.05)	379 (±9)	0.32

Si/Al and Al content determined by the ICP-OES method; specific surface area (S<sub>BET</sub>) and pore volume determined by low-temperature nitrogen sorption. C<sub>A</sub>—surface concentration of acid sites, determined by the NH<sub>3</sub>-TPD method; MCM-41—calcinated sample used for preparation of the catalysts by the impregnation and TIE methods; \*—experimental error is about ±0.01 wt.%.

The examples of the nitrogen adsorption-desorption isotherms recorded for the samples with the highest aluminum content, deposited by different methods, are presented in Figure 2. The isotherms are classified according to the IUPAC standards as type IVb

(Figure 2) and are characteristic of MCM-41-type mesoporous materials [24,25]. A steep increase in nitrogen uptake at a relative pressure of 0.15–0.35 is assigned to the capillary condensation of nitrogen inside the mesopores, while an increase in adsorbed volume above  $p/p_0 = 0.9$  is possibly related to the nitrogen condensation in the interparticle spaces. The isotherms do not exhibit hysteresis loops, indicating that the adsorption process is completely reversible. The type of IVb isotherm, with no hysteresis loop, is characteristics of mesoporous materials with pore diameters below 4 nm [25].

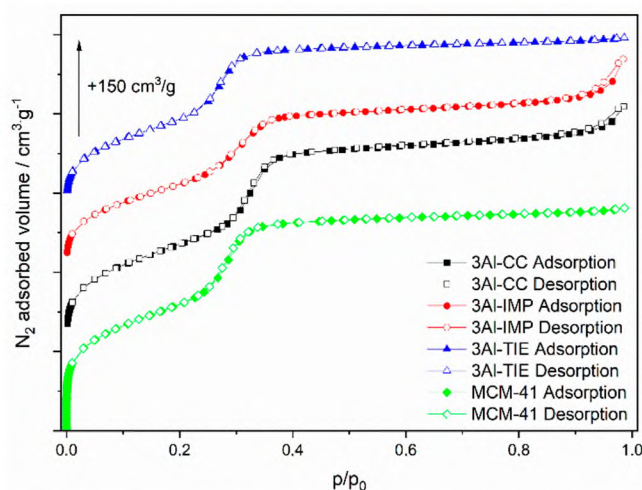


**Figure 2.** Nitrogen adsorption-desorption isotherms of MCM-41, modified with aluminum by different methods, and for pure silica MCM-41.

Profiles of pore size distribution (PSD) prove the high uniformity of pore size in the studied samples (examples of PSD profiles are presented in Figure 3). In the case of all studied samples, the maximum of PSD is located at about 3.3–3.6 nm. This maximum is significantly less intense for the samples obtained by the impregnation method in comparison to the samples produced by the co-condensation and TIE methods. In the case of the impregnation method, it is possible that part of aluminum was deposited into the MCM-41 pores in the form of small  $\text{Al}_2\text{O}_3$  aggregates (in which the size of crystallites is below the detection limit of the XRD method). In the samples obtained by the co-condensation method, alumina species were incorporated into the silica walls of MCM-41, while in the case of the TIE method, aluminum was deposited in the form of a much better dispersed species, compared to the impregnation method. Thus, in the samples produced by the co-condensation and TIE methods, a decrease in the PSD profiles was not observed.

The specific surface area ( $S_{\text{BET}}$ ) and pore volume of the samples are compared in Table 1. The samples obtained by the co-condensation method were characterized by a surface area above  $1100 \text{ m}^2 \cdot \text{g}^{-1}$  and a pore volume of about  $1 \text{ cm}^3 \cdot \text{g}^{-1}$ . In the case of the samples modified with aluminum by the impregnation and TIE methods, their specific surface area and porosity gradually decreased with increasing aluminum loadings. This effect is attributed to the accumulation of aluminum species inside the pores of these materials.

The surface acidity of the samples was analysed using the method of the temperature-programmed desorption of ammonia ( $\text{NH}_3$ -TPD). Ammonia desorption profiles are presented in Figure 4, while the concentrations of surface acid sites in the samples are compared in Table 1 (it was assumed that one ammonia molecule was bound to one acid site). Pure silica MCM-41 presented no surface acidity (results not shown); thus, the acid sites are related to the presence of aluminum species in the samples. As it can be seen, for all series of the samples, the content of the surface acid sites increases with the increasing aluminum content (Table 1). The samples obtained by the co-condensation method presented the lowest acid sites concentrations. This is not surprising, considering the relatively low content of the introduced aluminum species (Table 1). Moreover, in the case of these samples, a



portion of the aluminum was occluded inside the silica walls and was not exposed on the sample surface. The molar ratio of acid site concentration to aluminum content, presented in Table 1, is about 0.20 for the sample with the lowest aluminum loading, 1Al-CC, and this ratio decreased for the samples along with the increasing aluminum contents. In the case of impregnation method, aluminum species were deposited on the silica surface, which resulted in the increased concentration of acid sites in this series of samples in comparison to the catalysts obtained by the co-condensation method. On the other hand, the ratio of acid site concentration to aluminum content in this series of samples is similar, or even slightly lower, compared to the catalysts obtained by the co-condensation method. As was previously proposed, the impregnation method possibly resulted in the deposition of more aggregated aluminum species, thus decreasing the accessibility of surface  $\text{Al}^{3+}$  cations. The samples obtained by the TIE method presented the highest acid site concentrations and the highest ratio of acid site concentration to aluminum content (Table 1), indicating that the TIE method results in the deposition of aluminum in the form of highly dispersed surface species.

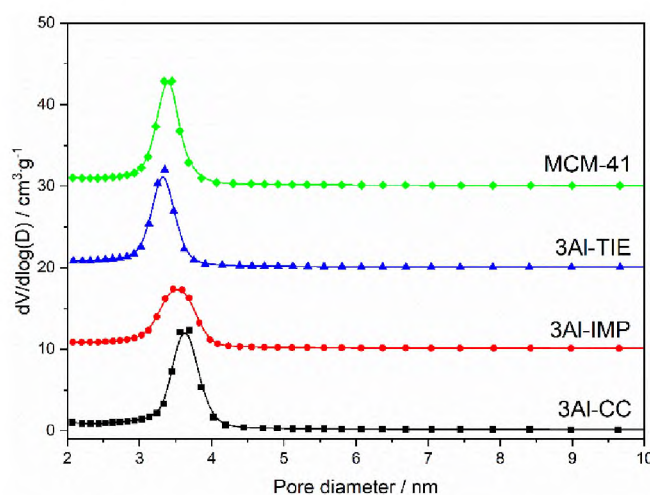


**Figure 3.** Pore size distribution (PSD) determined for MCM-41, modified with aluminum by different methods, and for pure silica MCM-41.

Ammonia desorption profiles are spread out along the temperature range of 70–620 °C, indicating the presence of acid sites of various strengths (Figure 4). The desorption profile obtained for the 1Al-CC sample consists of at least two maxima located at about 160 and 290 °C and assigned to the presence of relatively weaker and stronger acid sites (Figure 4A). An increase in aluminum loading, 2Al-CC and 3Al-CC, resulted in a shift of these peaks to about 185 and 315 °C, indicating an increase in the strength of the acid sites. A similar ammonia desorption profile, with maxima at about 185 and 295 °C, was obtained for the 1Al-IMP sample (Figure 4B). An increase in the aluminum content, 2Al-IMP and 3Al-IMP, deposited by the impregnation method resulted in desorption profiles with one asymmetric maximum at about 225–245 °C, which is possibly a superposition of the peaks related to the weaker and stronger acid sites. Similar ammonia desorption profiles were noted for mesoporous silica modified with aluminum using the TIE method (Figure 4C). The main maximum is located at 210–220 °C, with the shoulder at about 330 °C. A comparison of the ammonia desorption profiles obtained for the silica samples modified with aluminum by the impregnation (Figure 4B) and TIE (Figure 4C) methods shows only small differences in the acid strength of the different aggregated aluminum species. On the other hand, the deposition of aluminum using the TIE method resulted in more dispersed species and therefore, a higher concentration of acid sites compared to the samples obtained by the impregnation method.

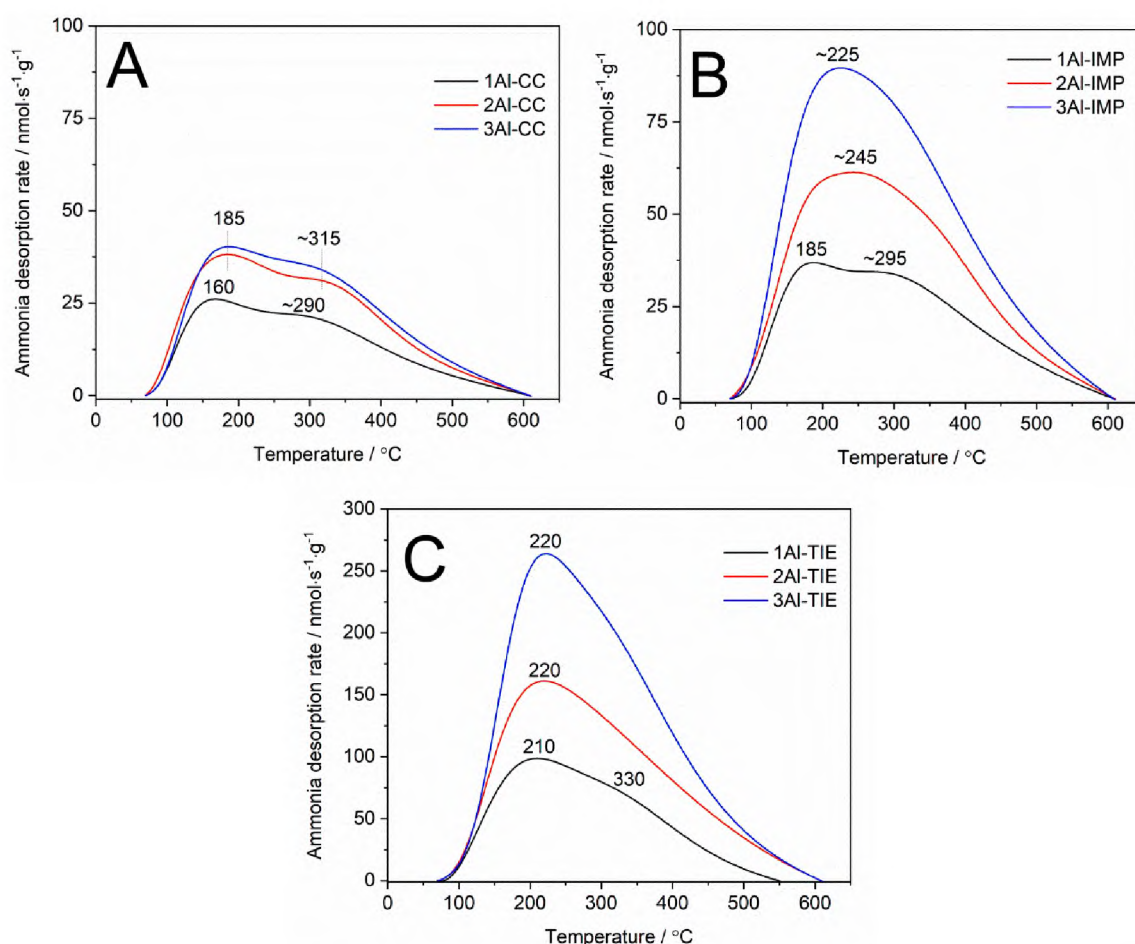


**Figure 4.** NH<sub>3</sub>-TPD profiles of MCM-41 modified with aluminum by co-condensation (A), impregnation (B) and TIE (C) methods.

The conversion of methanol to DME in the catalyst, in the absence or presence of pure silica MCM-41, was not observed (Supplementary Materials, Figure S1). However, at temperatures above 300 °C, methanol was partially converted into CO, CH<sub>4</sub>, and formaldehyde. The results of the catalytic studies regarding the reaction of methanol to dimethyl ether (DME) conversion in the presence of MCM-41 modified with aluminum are shown in Figure 5. As can be seen, the catalytic activity of the studied samples depends on the surface concentration of the acid sites generated by the deposition of aluminum species. The catalysts obtained by the co-condensation method presented relatively low activity; however, an increase in the aluminium loading in the samples resulted in their catalytic activation in the reaction of methanol to DME dehydration (Figure 5A). The catalyst obtained by the impregnation method were found to be more active compared to the samples produced by the co-condensation method. It can be seen that the activity of the catalysts of this series increases with the increase in aluminum loading (Figure 5B). Due to thermodynamic limitations (see the dashed line in Figure 5C), the complete methanol to DME conversion was not achieved at higher temperatures [26]. The series of the catalysts obtained by the TIE method presented the highest activity regarding methanol dehydration (Figure 5C); however, also in this case, the content of deposited aluminum determined the catalytic performance of the samples. Thus, it could be concluded that the surface concentration of the acid sites generated by the presence of aluminum in the samples determines their catalytic performance in the studied reaction. Aluminum was deposited on the surface of MCM-41 in the form of differently aggregated species. In the case of the catalysts obtained by the impregnation method, a significant contribution of small, aggregated aluminum species could be expected, while the application of the TIE method resulted in the deposition of



additional dispersed aluminum species. To compare the average activity of the active sites present in the catalysts, the turnover frequency (TOF) values for the reaction conducted at 250 °C were determined (Figure 5). It was assumed that each acid site, determined by the  $\text{NH}_3$ -TPD measurements (Table 1), played a role in the catalytically active site. As it can be seen (Figure 5B), the active sites in the catalysts obtained by the impregnation method are more catalytically active in comparison to the active sites in the catalysts produced by the TIE method (Figure 5C). Thus, it could be supposed that the acid sites associated with the aggregated aluminum species are more efficient in methanol conversion than the highly dispersed aluminum species. However, the TOF values decreased with increasing aluminum loading (Figure 5B,C), which could lead to the opposite conclusion. Thus, the problem of aluminum species aggregation and its role in methanol dehydration seems to be much more complex, thus requiring additional study. The selectivity of the reaction to DME at temperatures below 325 °C for all studied catalysts is 100% (no side products were detected). For the tests at temperatures of 325 and 350 °C, small amounts of formaldehyde (FA), carbon monoxide, and methane were detected. For the most active catalyst, 3Al-TIE, the selectivity to side products (FA + CO +  $\text{CH}_4$ ) was 1.2% at 325 °C and 3.6% at 350 °C. For the other studied catalysts, the selectivity to side products was lower than for 3Al-TIE.

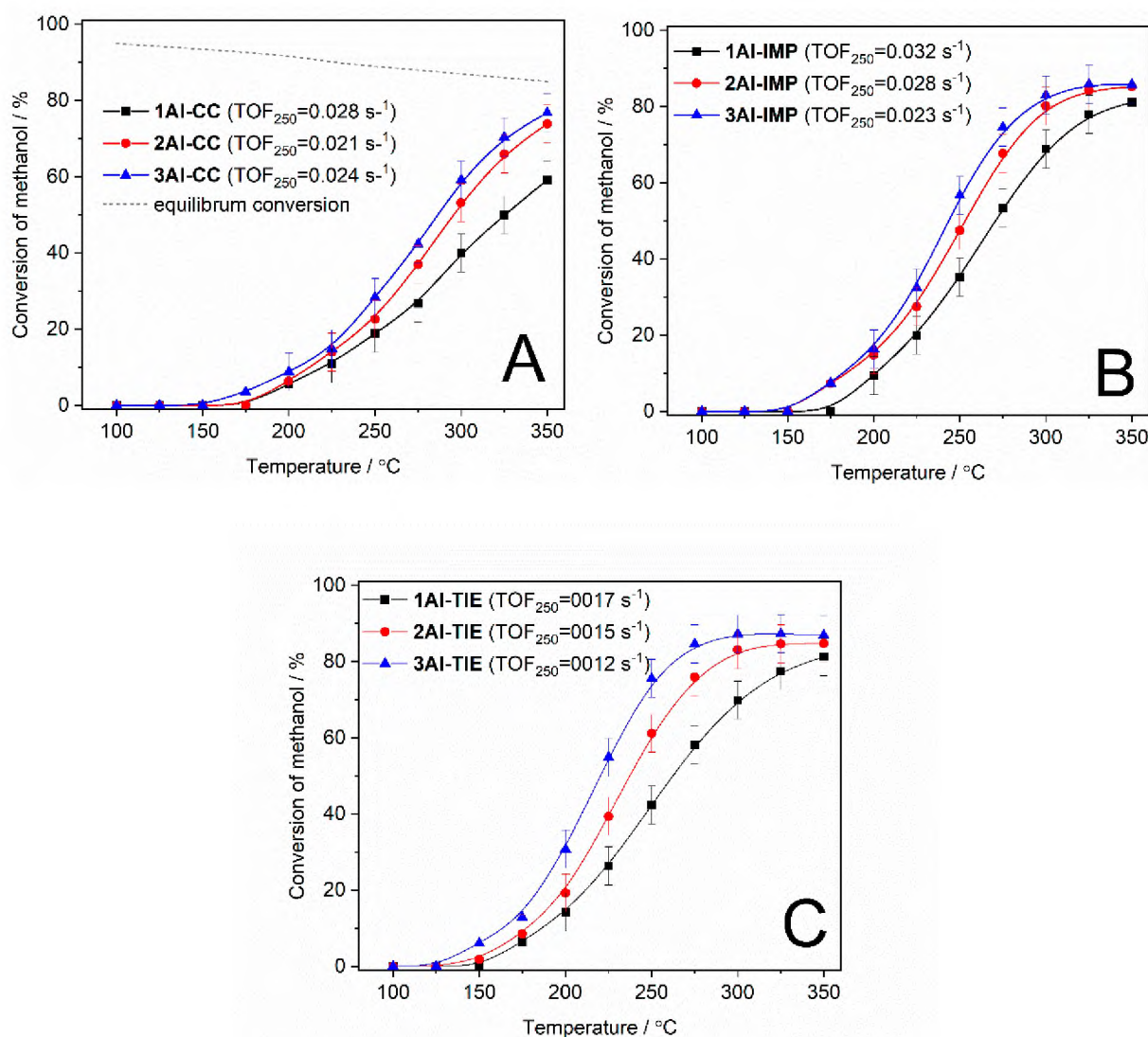


**Figure 5.** Results of the catalytic tests in the reaction of methanol to DME dehydration in the presence of MCM-41 modified with aluminum by the co-condensation (A), impregnation (B), and TIE (C) methods.

The stability of the most active catalyst, 3Al-TiE, under reaction conditions was verified by subsequent catalytic runs. The standard catalytic test was performed. After reaching 350 °C, the reactor was cooled down to 100 °C under a flow of pure helium. Then, the flow of helium was changed to the flow of the reaction mixture, and the next catalytic run was initiated. This procedure was repeated four times. As it can be seen in Figure 6A, the methanol conversion profile for the second run is shifted in the direction of higher temperatures by an increase of about 10–15 °C in comparison to the conversion profile obtained for the first run. The results of the subsequent catalytic cycles (runs 3 and 4) are very similar to the methanol conversion profile obtained in the second cycle. This indicates that the most intense catalyst deactivation occurs for the fresh catalyst. The catalyst after four catalytic runs was black (Figure 7C,D), clearly showing the formation of carbon deposits under the reaction conditions. To verify the content and stability of the carbon deposits formed under the reaction conditions, the catalyst sample after four catalytic runs was analyzed using the thermogravimetric method under a flow of air (Figure 7). The drop in mass in the low-temperature range is associated with the removal of water physically absorbed on the catalyst surface, while the step in the TG profile at 450–650 °C is related to the burning of the carbon deposits formed on the catalyst under reaction conditions (Figure 7A). The DTG profile, presented in Figure 7B, shows the maximum efficiency of water removal, as well as carbon deposit incineration. Another series of catalytic runs for the 3Al-TiE catalysts is presented in Figure 6B. In this case, after each catalytic run, the reactor was heated to 550 °C, and then the catalyst sample was treated under a flow of air for 1 h. Subsequently, the reactor was cooled to 100 °C, and the next catalytic run was conducted. This procedure was repeated 3 times (Figure 6B). As can be seen, the methanol conversion profiles obtained for all runs are very similar, indicating that the procedure applied for the catalyst regeneration is effective. The deactivation effect is observed only after the first catalytic run, and it is not very significant (Figure 6A). In the subsequent runs, no significant changes in the catalyst activity were observed. Thus, a more economical mode of the MTD process with the use of the studied catalyst could be employed by conducting the process without regeneration cycles. Of course, this proposal requires verification by additional studies.

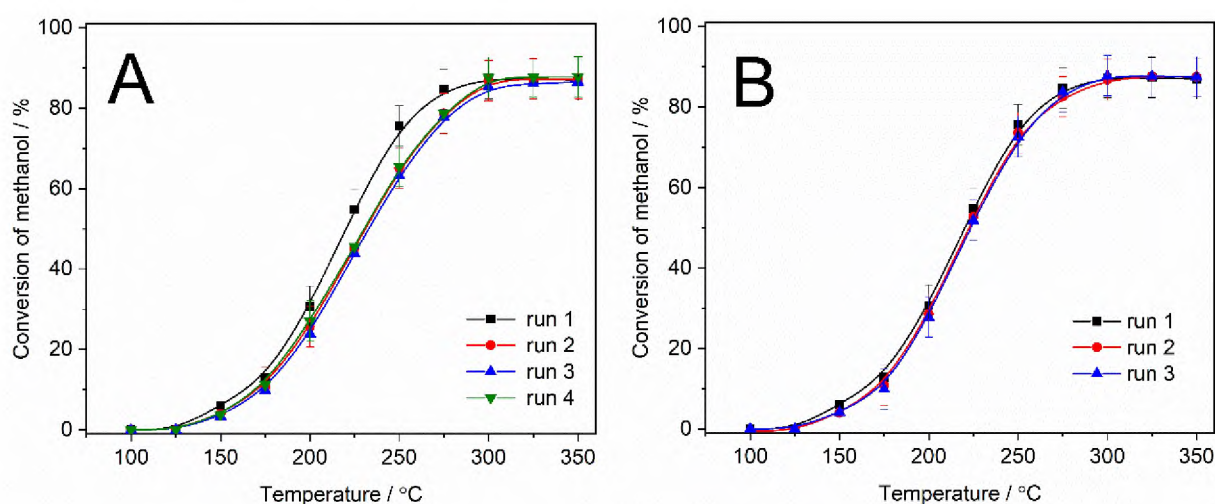


**Figure 6.** Results of the subsequent catalytic tests in the reaction of methanol to DME dehydration in the presence of the 3Al-TiE catalyst: (A) runs without catalyst regeneration, (B) runs with catalyst regeneration.



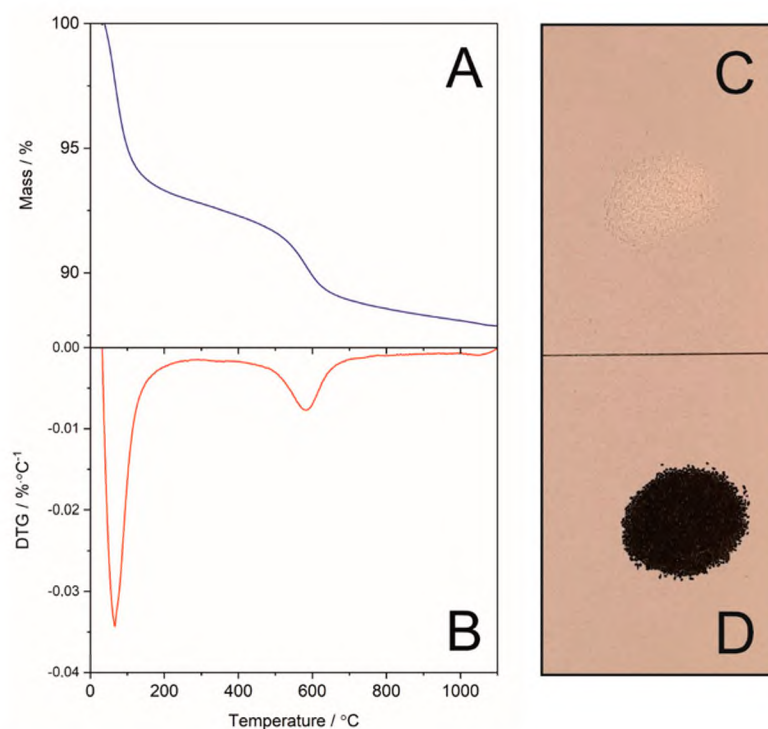


**Figure 7.** Thermogravimetric (TG) analysis of the 3Al-TIE sample after four catalytic runs. (A) TG profile, (B) DTG profile, (C) photographs of fresh and (D) used (after 4 catalytic runs) 3Al-TIE catalysts.

### 3. Materials and Methods

#### 3.1. Synthesis of Silica MCM-41

The procedure used for the synthesis of MCM-41-type mesoporous silica was presented in our previous paper [27]. Cetyltrimethylammonium chloride (CTMACl, Sigma-Aldrich, St. Louis, MO, USA), used as porous structure directing agent, and an aqueous solution of ammonia ( $\text{NH}_3 \cdot \text{H}_2\text{O}$ , Avantor/POCH, Gliwice, Poland) were introduced into distilled water. The obtained mixture was stirred at room temperature (RT) for 30 min, and then tetraethyl orthosilicate (TEOS, Sigma-Aldrich), used as a silica source, was added dropwise. The obtained slurry, with the molar ratio of 1 TEOS: 0.16 CTMACl: 2.76  $\text{NH}_3 \cdot \text{H}_2\text{O}$ : 140.13  $\text{H}_2\text{O}$ , was stirred for 1 h at RT and then separated by filtration. The obtained solid product was washed with distilled water and dried overnight at 60 °C. The obtained sample of the MCM-41 precursor is denoted as MCM-41(P).

#### 3.2. Deposition of Aluminum by the Impregnation Method

The first series of the catalysts was obtained by the incipient wetness impregnation method. The MCM-41(P) sample was calcined under an air atmosphere at 550 °C for 8 h (with the linear temperature increased from RT to 550 °C of  $1 \text{ }^\circ\text{C} \cdot \text{min}^{-1}$ ) to remove organic surfactants of the pore system of MCM-41. In the next step, the sorption capacity of MCM-41 was determined by soaking of the mesoporous silica samples in distilled water. Considering the sorption capacity of MCM-41 and the intended aluminum loadings in the catalysts, the silica samples were soaked with the aqueous solutions of  $\text{Al}(\text{NO}_3)_3$  (Honeywell, Charlotte, NC, USA), with volume and concentrations corresponding to the introduction of 0.084, 0.168, and 0.251 g of  $\text{Al}(\text{NO}_3)_3$  per 1 g of dried MCM-41 silica, which should result in the samples containing, 1, 2, and 3 wt.% of aluminum, respectively. The obtained samples were dried at 60 °C overnight and calcined in an air atmosphere at 550 °C for 8 h (with the linear temperature increase rate of  $1 \text{ }^\circ\text{C} \cdot \text{min}^{-1}$ ). The catalysts of this series with the intended aluminum loading of 1, 2, and 3 wt.% are denoted as 1Al-IMP, 2Al-IMP, and 3Al-IMP, respectively.

### 3.3. Deposition of Aluminum by Template Ion-Exchange (TIE) Method

A total of 1 g of MCM-41(P) was dispersed in 50 mL of methanol solution of  $\text{Al}(\text{NO}_3)_3$  and intensively stirred under reflux at 70 °C for 3 h. To obtain samples with the intended final aluminum loadings of 1, 2, and 3 wt.%, the methanol solutions (50 cm<sup>3</sup>), containing 0.048, 0.097 and 0.142 g of  $\text{Al}(\text{NO}_3)_3$  (Honeywell), respectively, were used for 1 g of freshly prepared MCM-41 (non-calcined). The concentrations of the solutions used were determined considering that freshly synthesized MCM-41 contains 42 wt.% of organic matter (determined by the thermogravimetric method). The obtained samples were washed with pure methanol, dried at 60 °C overnight, and calcined in an air atmosphere at 550 °C for 8 h (with the linear temperature increase of 1 °C·min<sup>-1</sup>) to remove residual surfactants from the pore system of the mesoporous silica. The catalysts of this series with the intended aluminum content of 1, 2, and 3 wt.% are denoted as 1Al-TIE, 2Al-TIE, and 3Al-TIE, respectively.

### 3.4. Synthesis of Al-MCM-41 by the Co-Condensation Method

The third series of the catalysts was obtained by the co-condensation method. In the first step, hexadecyltrimethylammonium bromide (CTAB, Sigma-Aldrich), used as a porous structure directing agent, was introduced into the mixture of distilled water and aqueous solution of ammonia (Avantor/POCH) and intensively stirred at room temperature for 30 min. Then, the mixture of aluminum isopropoxide (AIP, Sigma-Aldrich) and tetraethyl orthosilicate (TEOS, Sigma-Aldrich), used as aluminum and silicon sources, respectively, were added to the reaction mixture dropwise. The molar AIP/TEOS ratios were 1/43, 1/21, and 1/13.7 to obtain the intended aluminum content of 1, 2, and 3 wt.% in the final samples. The reaction mixture was intensively stirred at RT for 1 h, and then the resultant slurry was filtered, washed with distilled water (to obtain pH = 7), and dried at 60 °C overnight. Finally, the samples were calcined at 550 °C for 6 h under an air atmosphere. The catalysts of this series, with the intended aluminum content of 1, 2, and 3 wt.%, are denoted as 1Al-CC, 2Al-CC, and 3Al-CC, respectively.

### 3.5. Catalyst Characterization

The aluminum and silicon contents of the samples were determined by the inductively coupled plasma optical emission spectrometry method (ICP-OES) using an iCAP 7000 instrument (Thermo Scientific, Waltham, MA, USA). Prior to the analysis, the solid samples were dissolved in a solution containing 6 mL  $\text{HNO}_3$  (67–69%), 2 mL  $\text{HCl}$  (30%), and 2 mL  $\text{HF}$  (47–51%) at 190 °C using a microwave digestion system, Ethos Easy (Milestone, Sorisole, Italy).

The diffraction patterns of the samples were recorded using a Bruker D2 Phaser diffractometer (Bruker, Billerica, MA, USA). The measurements were performed in the low  $2\theta$  angle range of 1–7° and the high  $2\theta$  angle range of 30–50°, with a step of 0.02°. The counting times of 5 s per step and 1 s per step were used for the low-angle and high-angle measurements, respectively.

Textural parameters, specific surface area, and pore volume of the Al-modified MCM-41 samples were determined by  $\text{N}_2$ -sorption at −196 °C using a 3Flex v.1.00 (Micromeritics, Norcross, GA, USA) automated gas adsorption system. Prior to the analysis, the samples were outgassed under vacuum at 350 °C for 24 h. Their specific surface area ( $S_{\text{BET}}$ ) was determined using the BET model, while the pore size distribution (PSD) profiles were determined by the analysis of the adsorption branch of the isotherm using the BJH model. The pore volume ( $V_{\text{T}}$ ) was estimated by means of the total amount of adsorbed  $\text{N}_2$  at the relative  $p/p_0$  pressure of 0.98.

The surface acidity of the samples was analyzed by the temperature-programmed desorption of ammonia ( $\text{NH}_3$ -TPD) method. The measurements were performed in a flow quartz microreactor system connected directly to a quadrupole mass spectrometer (QMS, PREVAC, Rogów, Poland) used as detector. The flow rate and composition of the gas mixture was adjusted and controlled by mass flow controllers (Brooks Instrument, Hatfield,



PA, USA). The catalyst sample (50 mg) was placed into microreactor and outgassed in a flow of pure helium at 550 °C for 30 min. Then, the microreactor was cooled to 70 °C, and the sample was saturated in a flow of gas mixture containing 1 vol.% NH<sub>3</sub> diluted in helium (flow rate of 20 mL·min<sup>-1</sup>) for about 2 h. Then, to remove the physisorbed forms of ammonia from the samples, the microreactor was purged in a helium flow until a constant base line level ( $m/z = 16$ ) was attained. Ammonia desorption was carried out with a linear heating rate of 10 °C·min<sup>-1</sup> under a flow of pure helium (20 mL·min<sup>-1</sup>). The calibration of the QMS detector with a commercial mixture allowed for the recalculation of the detector signal into the rate of ammonia desorption.

The most active catalyst after the catalytic runs was thermogravimetry (TG) analyzed. The TG measurement was obtained with the using TGA/DSC 3+ (Mettler Toledo, Greifensee, Switzerland). The TG and DTG profiles were obtained under a flow of synthetic air (80 mL·min<sup>-1</sup>), with the linear temperature increase of 20°·min<sup>-1</sup> in the temperature range of 30–1100 °C.

### 3.6. Catalytic Studies

The MCM-41 samples modified with alumina were tested regarding the role of the catalysts for methanol dehydration to dimethyl ether (DME). Prior to the catalytic tests, the catalyst powder was pressed, crushed, and then sieved to obtain the grain fraction of 250–315 µm. The catalyst sample (100 mg) was placed in a flow fixed-bed quartz microreactor on a quartz wool plug and outgassed in a flow of pure helium (20 mL·min<sup>-1</sup>) at 550 °C for 50 min. The catalytic test was carried out in the temperature range of 125–350 °C with a heating rate of 10 °C·min<sup>-1</sup> using a gas mixture containing an alcohol (3.9 vol. % of methanol determined by their volatility at 0 °C, which was the saturation temperature) diluted in helium with the total flow rate of 20 mL·min<sup>-1</sup>. The concentrations of reactants were analyzed using a gas chromatograph (SRI 8610C, SRI Instruments, Earl St. Torrance, CA, USA) equipped with a methanizer and an FID detector. The operating temperature of the chromatography column (Merck, St. Louis, MO, USA) was 120 °C.

## 4. Conclusions

Three series of MTD catalysts obtained by the deposition of aluminum species onto MCM-41-type mesoporous silica were prepared. The catalysts obtained by the template ion-exchange method (TIE) presented significantly better catalytic activity for methanol to DME dehydrogenation comparing to the samples produced by the impregnation and co-condensation methods. On the other hand, the analysis of catalytic activity related to catalytic centers (TOF values) showed a higher activity for such sites in the catalysts obtained by the impregnation method. Thus, aggregated aluminum species possibly present a higher activity in the methanol to DME conversion than do the highly dispersed aluminum species. The overall reaction efficiency in the case of the catalysts obtained by the TIE method was explained by more effective deposition of the highly dispersed aluminum species on the surface of the MCM-41 support by TIE method, yielding a higher surface concentration of acid sites than in the case of the catalysts produced by the impregnation and co-condensation methods. Under the conditions of the catalytic test, the formation of carbon deposits, which decreased the catalytic activity of the catalysts, was observed (for the 3Al-TIE-shift of the conversion profile, the temperatures increased by about 10–15 °C). The most intensive deactivation of the catalysts occurred for the fresh samples (first catalytic cycle). The treatment of the catalysts under a flow of air at 550 °C resulted in their complete regeneration.

**Supplementary Materials:** The following supporting information can be downloaded at: <https://www.mdpi.com/article/10.3390/catal12111324/s1>, Figure S1: Results of methanol conversion in an empty reactor and in the presence of pure silica MCM-41.



**Author Contributions:** Conceptualization, L.C.; methodology, N.S., A.K., Z.P. and L.C.; investigation, N.S., A.K. and Z.P.; data curation, L.C.; writing—original draft preparation, L.C.; writing—review and editing, L.C.; visualization, N.S. and L.C.; supervision, L.C.; project administration, L.C. All authors have read and agreed to the published version of the manuscript.

**Funding:** This research was funded by the National Science Center (Poland), grant number 2018/31/B/ST5/00143.

**Data Availability Statement:** Experimental data will be available for the request.

**Conflicts of Interest:** The authors declare no conflict of interest.

## References

1. Putrasari, Y.; Lim, O. Dimethyl Ether as the Next Generation Fuel to Control Nitrogen Oxides and Particulate Matter Emissions from Internal Combustion Engines: A Review. *ACS Omega* **2022**, *7*, 32–37. [[CrossRef](#)] [[PubMed](#)]
2. Azizi, Z.; Rezaeimanesh, M.; Tohidian, T.; Rahimpour, M.R. Dimethyl Ether: A Review of Technologies and Production Challenges. *Chem. Eng. Process. Process Intensif.* **2014**, *82*, 150–172. [[CrossRef](#)]
3. Tokay, K.C.; Dogu, T.; Dogu, G. Dimethyl ether synthesis over alumina based catalysts. *Chem. Eng. J.* **2012**, *184*, 278–285. [[CrossRef](#)]
4. Abu-Dahrieh, J.; Rooney, D.; Goguet, A.; Saih, Y. Activity and deactivation studies for direct dimethyl ether synthesis using CuO-ZnO-Al<sub>2</sub>O<sub>3</sub> with NH<sub>4</sub>-ZSM-5, HZSM-5 or gamma-Al<sub>2</sub>O<sub>3</sub>. *Chem. Eng. J.* **2012**, *203*, 201–211. [[CrossRef](#)]
5. Frazão, C.J.R.; Walther, T. Syngas and Methanol-Based Biorefinery Concepts. *Chem. Ing. Tech.* **2020**, *92*, 1680–1699. [[CrossRef](#)]
6. Stiefel, M.; Ahmad, R.; Arnold, U.; Döring, M. Direct synthesis of dimethyl ether from carbon-monoxide-rich synthesis gas: Influence of dehydration catalysts and operating conditions. *Fuel Process. Technol.* **2011**, *92*, 1466–1474. [[CrossRef](#)]
7. Alamolhoda, A.; Kazemeini, M.; Zaherian, A.; Zakerinasab, M.R. Reaction kinetics determination and neural networks modeling of methanol dehydration over nano  $\gamma$ -Al<sub>2</sub>O<sub>3</sub> catalyst. *J. Ind. Eng. Chem.* **2012**, *18*, 2059–2068. [[CrossRef](#)]
8. Kipnis, M.A.; Samokhin, P.V.; Volnina, E.A.; Lin, G.I. Surface reactions of dimethyl ether on  $\gamma$ -Al<sub>2</sub>O<sub>3</sub>: 1. Adsorption and thermal effects. *Kinet. Catal.* **2014**, *55*, 456–462. [[CrossRef](#)]
9. Palcic, A.; Catizzzone, E. Application of nanosized zeolites in methanol conversion processes: A short review. *Curr. Opin. Green Sustain. Chem.* **2021**, *27*, 100393. [[CrossRef](#)]
10. Marosz, M.; Kowalczyk, A.; Gil, B.; Chmielarz, L. Acid-treated Clay Minerals as Catalysts for Dehydration of Methanol and Ethanol. *Clays Clay Miner.* **2020**, *68*, 23–27. [[CrossRef](#)]
11. Chmielarz, L.; Kowalczyk, A.; Skoczek, M.; Rutkowska, M.; Gil, B.; Natkański, P.; Radko, M.; Motak, M.; Dębek, R.; Ryczkowski, J. Porous clay heterostructures intercalated with multicomponent pillars as catalysts for dehydration of alcohols. *Appl. Clay Sci.* **2018**, *160*, 116–125. [[CrossRef](#)]
12. Schnee, J.; Gaigneaux, E.M. Lifetime of the H<sub>3</sub>PW<sub>12</sub>O<sub>40</sub> heteropolyacid in the methanol-to-DME process: A question of pre-treatment. *Appl. Catal. A Gen.* **2017**, *538*, 174–180. [[CrossRef](#)]
13. Ogródowicz, N.; Lalik, E.; Micek-Ilnicka, A. Alcohols dehydration in heterogeneous system—FTIR method development for quantitative determination of catalytic parameters. *Mol. Catal.* **2019**, *469*, 1–9. [[CrossRef](#)]
14. Peinado, C.; Liuzzi, D.; Ladera-Gallardo, R.M.; Retuerto, M.; Ojeda, M.; Peña, M.A.; Rojas, S. Effects of support and reaction pressure for the synthesis of dimethyl ether over heteropolyacid catalysts. *Sci. Rep.* **2020**, *10*, 8551. [[CrossRef](#)] [[PubMed](#)]
15. Hassanpour, S.; Yaripour, F.; Taghizadeh, M. Performance of modified H-ZSM-5 zeolite for dehydration of methanol to dimethyl ether. *Fuel Process. Technol.* **2010**, *91*, 1212–1221. [[CrossRef](#)]
16. Pogorielov, M.; Smyrnova, K.; Kyrylenko, S.; Gogotsi, O.; Zahorodna, V.; Pogrebnyak, A. MXenes—A New Class of Two-Dimensional Materials: Structure, Properties and Potential Applications. *Nanomaterials* **2021**, *11*, 3412. [[CrossRef](#)]
17. Pogrebnyak, A.D.; Postolnyi, B.; Marchenko, T.; Rudenko, P.; Marchenko, S. Enhancement of Mechanical, Electrical, and Chemical Properties of Polycarbonate-based Core-shell Composites by Modification with Single-walled Carbon Nanotubes. *High Temp. Mater. Process. Int. Q. High-Tech. Plasma Process.* **2021**, *25*, 53–64. [[CrossRef](#)]
18. Kowalczyk, A.; Świąć, A.; Gil, B.; Rutkowska, M.; Piwowarska, Z.; Borcuch, A.; Michalik, M.; Chmielarz, L. Effective catalysts for the low-temperature NH<sub>3</sub>-SCR process based on MCM-41 modified with copper by template ion-exchange (TIE) method. *Appl. Catal. B Environ.* **2018**, *237*, 927–937. [[CrossRef](#)]
19. Chmielarz, L.; Rutkowska, M.; Kowalczyk, A. Advances in Functionalization of Inorganic Porous Materials for Environmental Catalysis. *Adv. Inorg. Chem.* **2018**, *72*, 323–383.
20. Chmielarz, L.; Jankowska, A. Mesoporous silica-based catalysts for selective catalytic reduction of NO<sub>x</sub> with ammonia—Recent advances. *Adv. Inorg. Chem.* **2022**, *79*, 205–242.
21. Jankowska, A.; Chłopek, A.; Kowalczyk, A.; Rutkowska, M.; Mozgawa, W.; Michalik, M.; Liu, S.; Chmielarz, L. Enhanced catalytic performance in low-temperature NH<sub>3</sub>-SCR process of spherical MCM-41 modified with Cu by template ion-exchange and ammonia treatment. *Microporous Mesoporous Mater.* **2021**, *315*, 110920. [[CrossRef](#)]
22. Jankowska, A.; Kowalczyk, A.; Rutkowska, M.; Michalik, M.; Chmielarz, L. Spherical Al-MCM-41 Doped with Copper by Modified TIE Method as Effective Catalyst for Low-Temperature NH<sub>3</sub>-SCR. *Molecules* **2021**, *26*, 1807. [[CrossRef](#)] [[PubMed](#)]



23. Mendez, F.J.; Bastardo-Gonzalez, E.; Betancourt, P.; Paiva, L.; Brito, J.L. NiMo/MCM-41 catalysts for the hydrotreatment of polychlorinated biphenyls. *Catal. Lett.* **2013**, *143*, 93–100. [[CrossRef](#)]
24. Leofanti, G.; Padovan, M.; Tozzola, G.; Venturelli, B. Surface area and pore texture of catalysts. *Catal. Today* **1998**, *41*, 207–219. [[CrossRef](#)]
25. Thommes, M.; Kaneko, K.; Neimark, A.V.; Olivier, J.P.; Rodriguez-Reinoso, F.; Rouquerol, J.; Sing, K.S.W. Physisorption of gases, with special reference to the evaluation of surface area and pore size distribution (IUPAC Technical Report). *Pure Appl. Chem.* **2015**, *87*, 1051–1069. [[CrossRef](#)]
26. Diep, B.T.; Wainwright, M.S. Thermodynamic equilibrium constants for the methanol-dimethyl ether-water system. *J. Chem. Eng. Data* **1987**, *32*, 330–333. [[CrossRef](#)]
27. Kowalczyk, A.; Piwowarska, Z.; Macina, D.; Kuśtrowski, P.; Rokicińska, A.; Michalik, M.; Chmielarz, L. MCM-41 modified with iron by template ion-exchange method as effective catalyst for DeNOx and NH<sub>3</sub>-SCO processes. *Chem. Eng. J.* **2016**, *295*, 167–180. [[CrossRef](#)]